ARTICLE

High throughput production of microcapsules using microfluidics for self-healing in cementitious materials

Received 00th January 20xx,
Accepted 00th January 20xx

DOI: 10.1039/x0xx00000x

Lívia Ribeiro de Souza,*[a] Abir Al-Tabbaa [a]

Capsule-based self-healing of cementitious materials is an effective way of healing cracks, significantly extending the life of structures, without imposing changes for its incorporation into products during mixing. The methodologies currently being used for the development of capsules with liquid core as healing agent yield a wide range of size and shell thickness for the microcapsules, preventing a detailed assessment and optmisation of microcapsule size and its effects. Uniquely, microfluidics technology offers precise control over the size and shell thickness through the formation of double emulsions. The drawback is that only small quantities of material can be typically produced. Here, by using paralleled junctions in a microfluidic device, high throughput of material was produced, focusing for the first time on self-healing of cementitious materials. A microfluidic chip was assembled with 4 channels in parallel and selected hydrophobicity for the formation of the double emulsions. A coefficient of variation below 2.5% was observed in between the 4 junctions, demonstrating the formation of monodisperse capsules. The control over size and shell thickness by adjusting the flow rates was demonstrated, yielding capsules with 615-630 µm outer diameter and shell thickness varying between 50 and 127 µm. By using triethanolamine as a surfactant, capsules with an aqueous core were produced. Furthermore, by selecting PEA, an acrylate with low tensile strength, the capsules embedded in cement paste were successfully triggered by cracks. Capsules were successfully produced for continuous 7 h, with an inner and outer diameter of 500 ± 31 µm and 656 ± 9 µm, at a production rate of ~13g.h^{-1} and yielding around 80%. With these results, and considering up to 6 chips in parallel, up to 1.5kg per day could be produced. This demonstrates the huge potential of unique features of the microfluidic device to produce sufficiently large quantities of microcapsules for laboratory-scale assessment of self-healing performance.

Introduction

Inspired by the healing processes that occur in nature, the concept of self-healing in cementitious materials aims at decreasing repetitive and extensive maintenance cycles needed in infrastructures as well as extending its service life significantly contributing to the delivery of net zero by 2050.[1] The occurrence of cracks in cementitious infrastructure facilitates the ingress of water and chlorides which results in corrosion of reinforcing steel, causing deterioration in concrete.[2] With the use of self-healing in the concrete, when cracks are formed in the matrix, the healing takes place without the need for any external intervention.[3] This leads to recovery in transport properties and hence durability performance and, to some extent, to recovery in mechanical properties. Several methodologies have been applied to achieve such self-healing, including the enhancement in the autogenous capacity of cementitious materials to heal their own cracks through the addition of minerals,[4,5] fibres,[6] superabsorbent polymers (SAPs),[7]; and autonomic healing through vascular systems,[8,9] bacteria[10–12] and shape memory polymers.[13] However, the addition of these materials may lead to unwanted variations in the rheology during mixing and/or laborious changes to include the system during casting.[14] Capsule-based self-healing of cementitious materials, on the other hand, can easily be added during the mixing of cement and, at lower concentrations, with minimum effects on the mixture.[15,16] Once a crack is formed, the damage act as a trigger for releasing the encapsulated material. When the healing agent is released, it reacts and fills the crack and minimising the damage.[17] Examples of encapsulated healing agent for cementitious materials include liquids such as epoxy[18] and dissolved or emulsified minerals[19–21] and bacterial spores.[12] These materials have successfully been used to heal cracks up to 1 mm.[12]

A widely used strategy to produce capsules with liquid cores in large quantities is bulk emulsification followed by polymerisation of the shell. This methodology has been successfully used to encapsulate healing agents with a wide range of shells, such as poly(urea-formaldehyde),[22] polyurea,[16,23] gelatine-gum Arabic,[21] melamine formaldehyde,[12] and others. However, the inherent limitations of such bulk method is the production of capsules with a range of size,[24–26] shell thickness and structures, thus offering poor control of their release properties. Overall, ideal capsules should present suitable tensile strength and a good interfacial bond with the cementitious materials, as they would be easily triggered by

[a] *Department of Engineering, University of Cambridge, Cambridge CB2 1PZ, UK.*

cracks.[27] Other functionalities can also be programmed within the shell composition to create delivery systems whose release is controlled by variations in pH, chloride concentration and ultrasonic triggering.[28–30]

In the past few years, microfluidic production of double emulsions has gained attention due to the precise control over the size and shell thickness of the capsules, as well as a wide variety of shell properties[31]. However, the small scale of the chips and the low flow rates limit the large scale production. For one single chip, flow rates are typically around 0.5-1 $g.h^{-1}$ for the production of microcapsules.[31,32] These throughput values limit the amount of tests performed with the microcapsules. Particularly for self-healing in cementitious materials, a full spectrum of tests to evaluate the performance of capsules for the self-healing of cementitious materials, including capsules concentration, compressive strength, rheology, permeability and crack healing at different contents of microcapsules would need approximately 300 g of material.[15,16] To scale up the production, paralleled junctions in a microfluidic device have been explored, with early results placing 15-40 drop-makers consecutively to produce double emulsions.[33,34] However, for the reliable formation of water-in-oil-in-water double emulsions, a special pattern of wettability is necessary; in this case, a hydrophobic channel is used to form the water-in-oil emulsions, followed by and a hydrophilic channel is used for the double emulsion. Early studies circumvented the wettability issue by a selected change of geometry which allowed the hydrodynamic focusing of the middle phase.[33] In this case, the flow rates of middle and continuous phase are limited. Alternatively, emulsions with a core comprised of gas or with a core similar to the shell have also been investigated, as its production does not depend on selective surface wettability.[34,35] Recent advances on microfluidic systems have been used for larger-scale production of water-in-oil-in-water emulsions, producing up to ~50 $g.h^{-1}$.[36,37] Furthermore, a combination of large-scale production and machine learning can be used to minimise the need for a human operator checking the continuous production.[38,39]

Here, the high throughput production of microcapsules using microfluidics for mechanically triggered self-healing in the cementitious matrix was investigated. A microfluidic chip was developed with four junctions in parallel and suitable wettability for the formation of double emulsions. To demonstrate the monodisperse formation of double emulsions, the coefficient of variation between the double emulsions formed at the four junctions was investigated. Furthermore, the control over the size and shell thickness of the double emulsions was demonstrated. The double emulsion template was then used to produce capsules containing aqueous and organic core. In addition, capsules comprised of shell with low tensile strength and good interfacial bond with cementitious matrix were produced. In addition, capsules were produced continuously for 7 h, demonstrating the fabrication of sufficient material for laboratory-scale testing of self-healing performance. The size, shell thickness, core retention and yield of the continuous production were characterised. This study demonstrates the possibility of high throughput generation of microcapsules with controlled size and shell thickness for lab-scale assessment of self-healing performance in cementitious matrixes.

Results and discussion

Design of the chip.

The double emulsion template used for the formation of microcapsules was produced using a microfluidic chip, illustrated in Figure 1. During the design of the chip, four main factors were considered: (i) selected pattern of wettability, allowing the production of water-in-oil-in-water double emulsions; (ii) the uniform distribution of flow across each microfluidic junction; (iii) the size of the double emulsions to be ~500-600 μm, as this size is suitable for self-healing of cementitious materials; and (iv) maximised production, by including the largest number of junctions possible in a single chip. For the production of double emulsions with an aqueous (or organic) core and organic middle layer, the chip is composed of two parts connected together by a gasket: the first half has hydrophobic coating; after the gasket, the second part is glass, i.e., a hydrophilic material. In this way, the wettability of the chip was adapted to the production of water-oil-in-water double emulsions. The uniform distribution of liquids over droplet generators connected to a single distribution channel is achieved when the distribution channel is large enough so that the flow resistance R_D along the channel must be negligible compared to the flow resistance R_J through the microfluidic junction.[33] The resistance of a rectangular channel can be calculated by $R = 12\ \mu L/wh^3$ and the resistance of a circular channel can be calculated as $R=8\mu L/\pi a^4$ where μ is the dynamic viscosity of the fluid and l, w, h and d are the length, width, height and diameter of the channel, respectively. Resistors were added to the inner, middle and outer channel, as described in the experimental section, thus the presence of four junctions in the chip allows a uniform distribution of liquid over the chip. For the size of the double emulsions, it has been shown that the size of the droplets produced by flow focusing is comparable with the dimensions of the orifice [40]. Thus, the second junction was etched as 500 μm height and 510 μm width. Finally, considering the presence of the resistors, and width of the channels and the size of the clamps used in the commercially available Telos platform, the maximum number of junctions per chip was four. An advantage of this modular approach is the investigation of double emulsion production on a smaller scale (i.e., one single chip with four junctions), as well as the easy scale-up of the production. In this case, the channel dimensions play an important role on the uniform distribution of liquids throughout the different channels. Considering the dimensions of the channel on the commercially available Telos platform, and the resistors present in the chip, a system of

linear equations can be used to describe the flow rates in this ladder geometry, with 4 junctions branching out from each channel. In this case, for a system with N chips, the ratio of flow rates between Q_N and Q_0 is described in Equation 1:

$$\frac{Q_N}{Q_0} = 1 - \frac{4R_D}{R_f}\frac{(N-1)N}{2} \quad \text{(Eq. 1)}$$

Considering the design criteria that $Q_N/Q_0 \approx 0.99$, a maximum of 6 chips in parallel could be used with the chip presented in this work. To increase the value for N, the dimensions of the flow resistors and distribution channels may be tailored accordingly.

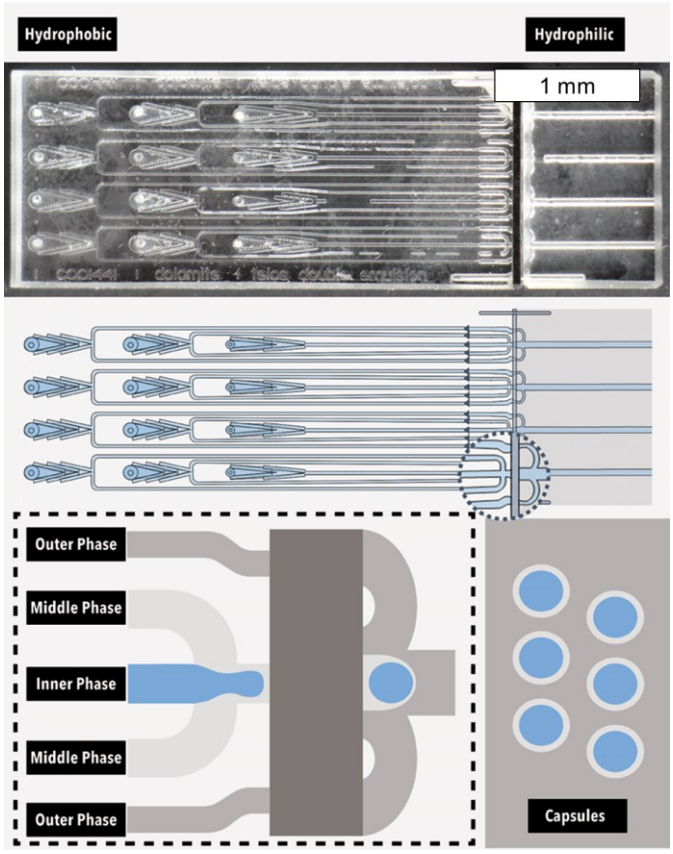

Figure 1 – A single microfluidic device for generation of monodisperse double emulsion. (top) Photography of the microfluidic device with a gasket separating the hydrophobic channels in the first half and hydrophilic second half. (middle) Schematic representation of a single microfluidic chip with four channels in parallel. (bottom left) Flow focusing junction where the inner, middle and outer phase form double emulsions. (bottom right) Microcapsules created by polymerising the double emulsion template.

Double emulsion formation

The size and shell thickness of the monodisperse double emulsion is easily fine-tuned according to the flow rates used for inner, middle, and outer phases. Considering the mechanism of formation of double emulsions in the dripping regime, the capillary number describes the main forces involved,[41] and the flow rates are the principal variables. Mineral oil was used as an inner fluid and ethylene glycol phenyl ether acrylate (PEA) was used as a middle fluid and PVA 5 wt% was used as the outer fluid, using flow rates of 130, 32 and 430 µL.min^{-1} for inner, middle and outer, respectively, as shown in Figure 2A. Highly monodispersed oil-in-oil-in-water double emulsions were formed in all four junctions with an outer diameter of 582 ± 4 µm for Junction 1, 604 ± 6 µm for Junction 2, 581 ± 5 µm for Junction 3 and 602 ± 6 µm for Junction 4. For each junction, the coefficient of variance (CV) was below 1%. The outer diameter for the 4 junctions combined was 590 ± 12 µm, with a CV below 2%, indicating the successful production of monodisperse double emulsions across the four junctions. The increase in CV for the combined junctions compared with the individual ones indicates small fluctuations in flow rate distribution between the junctions. The shell thickness of 24 ± 2 µm was obtained by measuring the difference between the inner and outer diameter.

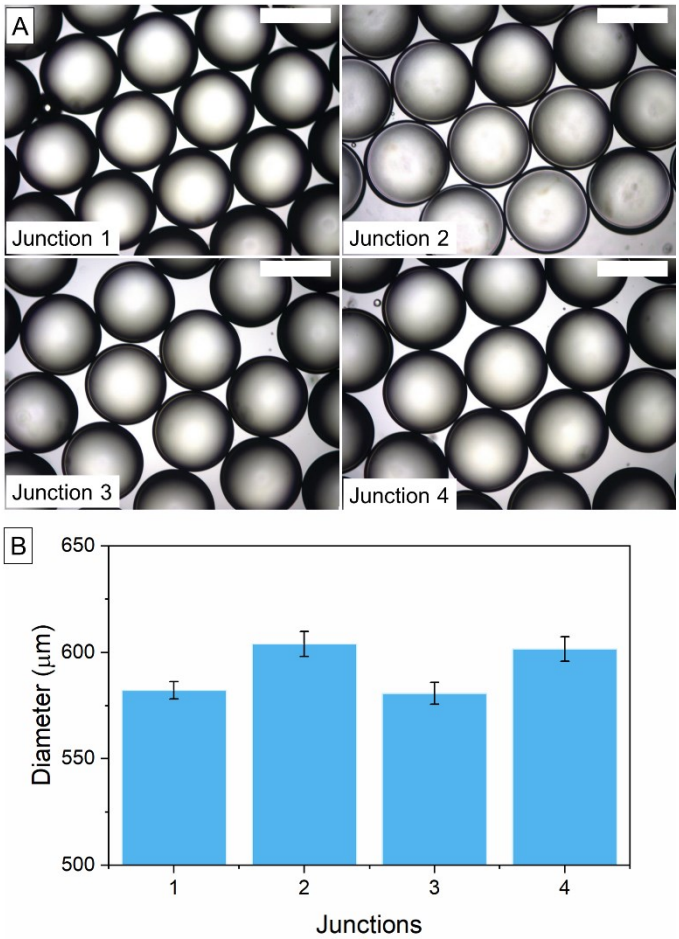

Figure 2 – (A) Optical microscope image of double emulsions template for capsules with organic core produced in the four parallelised junctions of the microfluidic device for a flow rate of 130, 32 and 430 µL min^{-1} for inner, middle and outer fluids. Scale bar indicates 500 µm. (b) Outer diameter of the capsules produced at different junctions.

The relative shell thickens (h) is defined as a function of the flow rate of the inner (q_{inner})and middle (q_{middle}) phases. By varying the flow rate of the inner phase, the shell thickness of the double emulsion can be defined as Equation (2):

$$h = \frac{D_{outer} - D_{inner}}{D_{outer}} = 1 - \left(1 + \frac{q_{middle}}{q_{inner}}\right)^{-1/3} \quad \text{(Eq. 2)}$$

Where D_{outer} is the outer diameter of the double emulsions and D_{inner} is the inner diameter.[41,42] The flow rate of mineral oil varied between 30 and 180 µL.min^{-1} whilst the flow rate of PEA was kept constant at 123 µL min^{-1}. Optical microscope images of the double emulsions produced in all four channels were measured and the outer diameter and inner diameter is shown Figure 3. The outer diameter for all the double emulsions varied between 615 to 630 µm with a coefficient of variation ~ 5% for all samples. The outer diameter is mainly determined by the outer flow rate, which was kept constant at 400 µL.min^{-1}. The inner diameter varied between 360 to 530 µm, with a shell thickness varying between 50 and 127 µm. Microcapsules' mean diameter around ~500-600 µm have been successfully demonstrated as effective for self-healing in cementitious materials.[15,16] Thus, producing double emulsion templates in this range of size is suitable for self-healing. Furthermore, the fine-tuning of the shell thickness can be used to increase the probability of physical triggering.

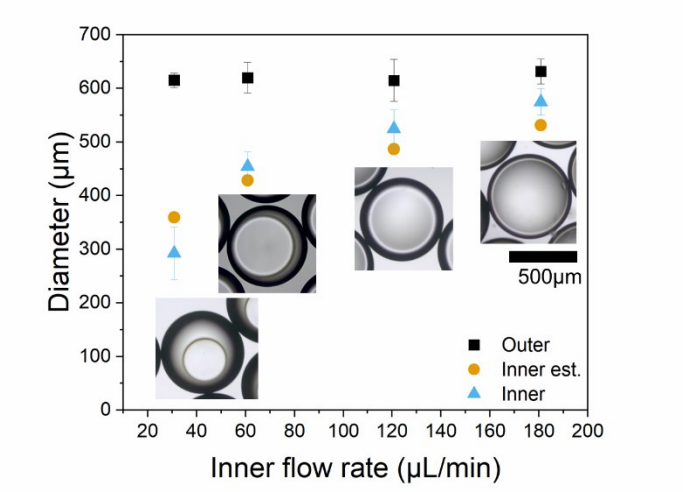

Figure 3 - Inner and outer diameter of double emulsions at a constant middle flow rate of 123 µL min^{-1} and an inner flow rate varying between 30 and 180 µL min^{-1} while the outer flow rate was kept constant at 400 µL min^{-1}.

Production of microcapsules with an aqueous core. Capsules with an aqueous-based core were produced using the microfluidic set-up, as aqueous cores are fundamental for several mechanisms of self-healing in cementitious matrices.[17,43] Double emulsions of water-in-oil-in-water (w/o/w) were produced using a mixture of triethanolamine in water as core, trimethylol-propane ethoxylate triacrylate as middle phase and PVA 5% as the outer phase. Figure 4a presents a typical optical microscopy image of the monodisperse double emulsions with an outer diameter of 597 ± 3 µm and inner diameter of 522 ± 2 µm. The flow rates were 60, 30 and 300 µL.min^{-1} for inner, middle and outer fluids, respectively. The triethanolamine contributed to increasing the viscosity in the inner fluid, thus increasing the drag of the inner phase and facilitating the formation of the double emulsion. In addition, it also acted as a non-ionic surfactant, reducing the interfacial tension between the core and the acrylate phase and stabilising the double emulsion. The double emulsion was polymerised and collected in a flask containing PVA 5%, immediately after the production. This is relevant to prevent the escape of the core during polymerisation. Figure 4b shows the formed microcapsules with a clear core-shell structure. Furthermore, the density of triethanolamine increased the density of the core, minimising the effects of mismatched density that may lead to off-centred cores using microfluidics.[44]

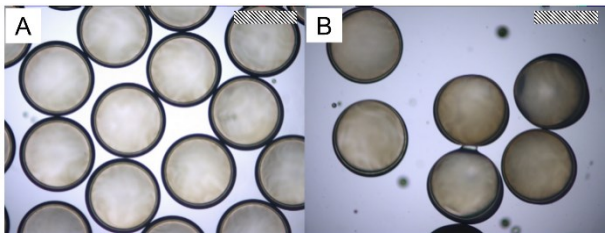

Figure 4 - Double emulsions (A) and capsules (B) produced with water-in-oil-water double emulsion. Scale bar represents 500 µm.

The maximum throughput for the production of double emulsions is dictated by the flow rates of the inner and middle fluid, however, it is also limited by the stability of the fluids. This is demonstrated with the water-in-oil-in-water double emulsion with PEA as the middle layer and PVA 5% as the outer liquid. To form the double emulsions, the flow rate was varied between 55-210 µL.min^{-1} for inner and 30-150 µL.min^{-1} for middle flow rate. The thickness of the middle layer increased with the increase of the middle fluid, as shown in the optical microscope images in Figure 5. In contrast, the thickness of the middle layer decreased with the increase of the inner fluid. Double emulsion throughput varied according to the used flow rates, ranging between 6 to 20 g.h^{-1} for a single chip. This value is comparable with recent reports in the literature, in which 20 mL.h^{-1} were produced with double emulsions.[37] However, using a modular platform, more chips may be placed in parallel, and this system allows a 6-fold increase in production. At flow rates 60 and 30 µL.min^{-1} for inner and middle fluids, the double emulsion was formed at the cross junction of the microfluidic channel in the dripping regime. With the increase of the inner and middle fluid, the throughput increases and the droplet formation changes to jetting and threading regimes[45,46], still robustly forming double emulsions. At inner flow rates above 150 µL.min^{-1} (for a middle flow rate of 110 µL.min-1), the stability of the system was significantly reduced as the flow is more likely to attach to the wall and not form double emulsions. Thus, aiming at high throughput, thinner shells, and stable formation of double emulsions, flow rates ranging between 60-120 µL.min^{-1} for inner and 30-110 µL.min^{-1} for middle were preferred.

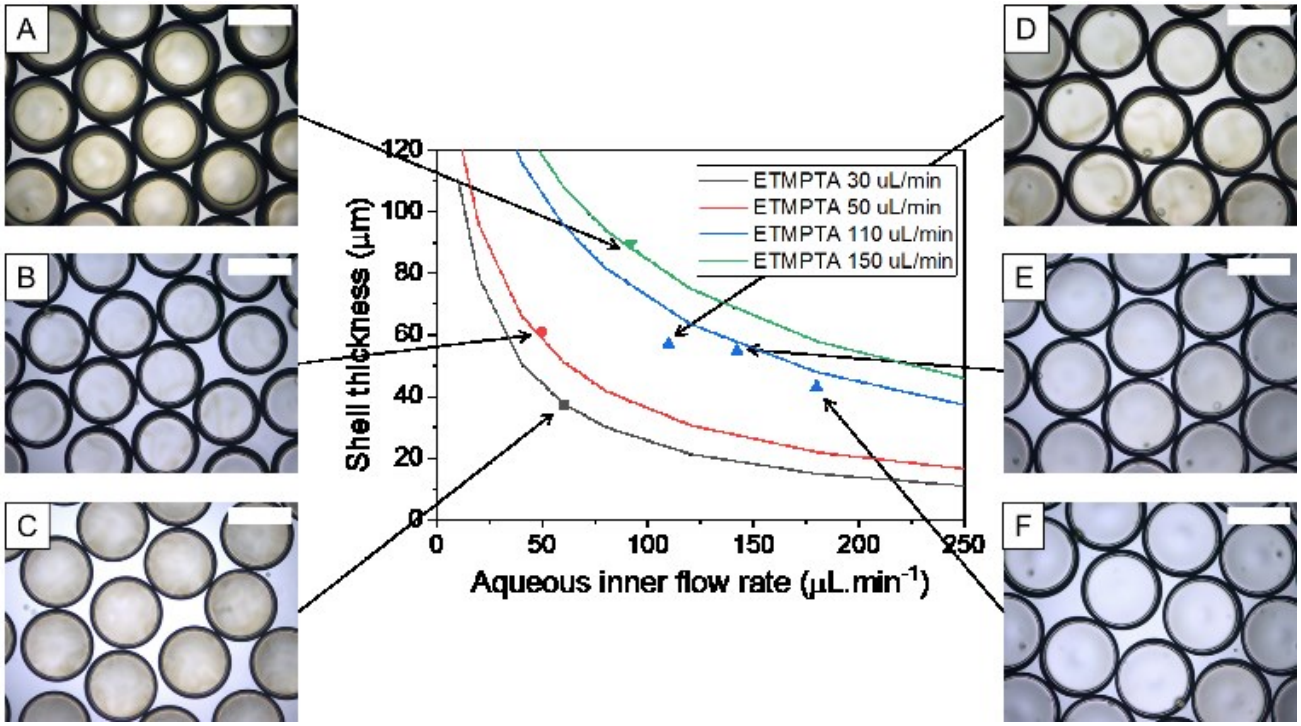

Figure 5 – Shell thickness of the water-in-oil-in-water (w/o/w) double emulsions tuned by controlling the inner and middle flow rate. Continuous lines indicate the estimated thickness of the middle layer for middle flow rates of 30 µL.min^{-1} and outer diameter (OD) of 597 µm (black), 50 µL.min^{-1} and OD of 560 µm (red), 110 µL.min^{-1} and OD of 662 µm (blue) and 150 µL.min^{-1} and OD of 633 µm (green). Symbols represent the measured middle layer thickness for double emulsions produced at a constant outer flow rates of 300 µL.min^{-1}. Scale bar represents 500 µm.

Production of microcapsules with shell for physical triggering. To be physically triggered when the crack is formed, the microcapsules need to present a good interfacial bond with cement paste and a low tensile strength to allow the rupture of the shell. Ethylene glycol phenyl ether acrylate (PEA) was selected as acrylate to be photopolymerised into shell due to the good interfacial bonding with cementitious materials and low tensile strength (~0.4 MPa)[47]. The PEA shelled microcapsules were produced using mineral oil as core, PEA as shell and PVA5% as outer material. Whilst the outer flow was kept constant at 400 µL.min^{-1}, the inner and middle flow were 90 and 150 µL.min^{-1}, respectively. The resulting double emulsion was produced with 600 µm in outer diameter and 90 µm of shell thickness (Figure 6A). Figure 6B shows the capsules collected in a solution of PVA 5 wt% whilst being polymerised on the fly, at production rate of ~14 g.h^{-1}. As the capsules are mostly comprised of a PEA, and acrylate with a density of 1.1 g.L^{-1}, the material precipitates instead of floating. This means the material does not agglomerate. Then the material was casted in cement paste – w/c at 0.45. After cracking, the capsules were ruptured and release the mineral oil as core, as observed with a stereoscope. In addition, scanning electron microscopy images show a very good bond between the capsule and the cement matrix, as shown in Figure 6C-D. And all capsules embedded in cement were ruptured upon crack formation. A previous investigation on encapsulation and behaviour in cement of capsules with ethylene glycol phenyl ether methacrylate and ethylene glycol phenyl ether acrylate reveal acrylates present a good interfacial bond with cement paste once compared with the methacrylates with same moieties. This hints at the importance of the structure of the PEA that allows a good interfacial bond with cement paste.

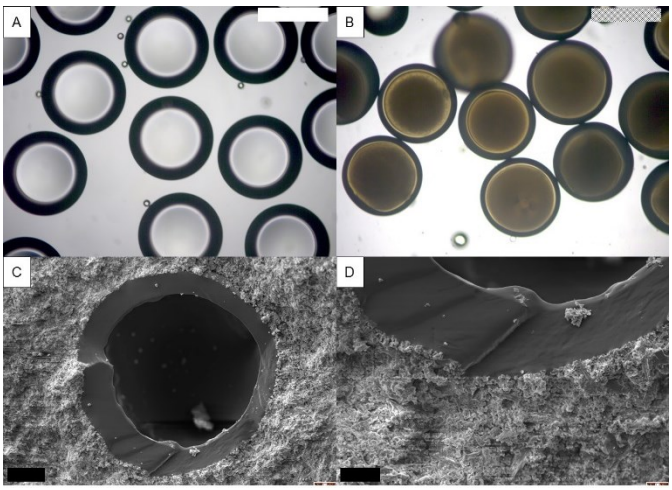

Figure 6 - Microcapsules produced for physical triggering self-healing in cementitious matrix. A) Optical image of double emulsion with mineral oil as core and PEA as shell. Scale bars: 500 µm B) Optical image of the microcapsules after the photopolymerisation of PEA. Scale bars: 500 µm C-D) SEM images of microcapsules embedded in cement paste; scale bars: 100 µm and 50 µm for C and D, respectively.

High throughput production of microcapsules. The production of large quantities of microcapsules is essential for lab assessment of the performance of capsule based self-healing materials. To demonstrate the use of parallelised junctions for the continuous production of double emulsions, microcapsules with PEA as shell and mineral oil as core were produced for 7 hours. Mineral oil, PEA and PVA 5wt% were pumped at the constant flow rate of 82, 130 and 400 µL.min^{-1}, respectively. The double emulsion was successfully formed in dripping regime at the cross junction, as shown in

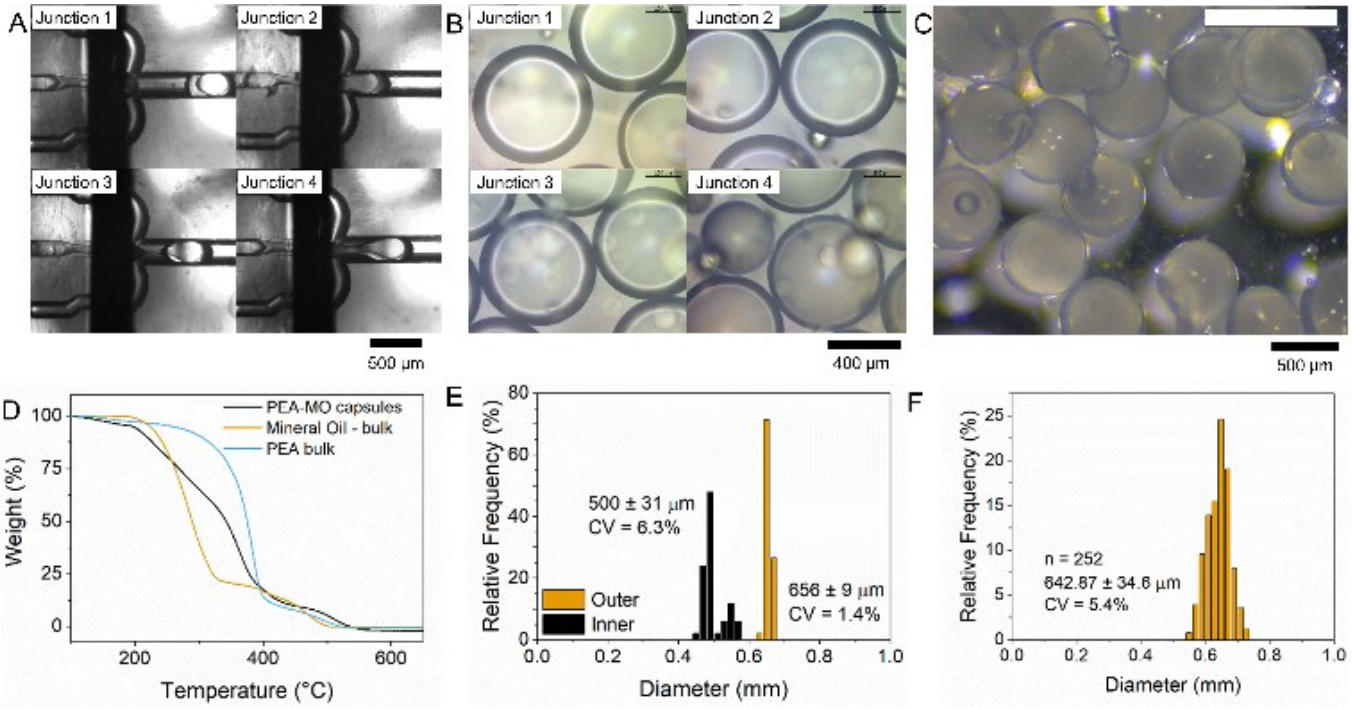

Figure 7A. The formed double emulsions are shown in the optical microscope image in

Figure 7B and the histograms indicating the size distributions are in

Figure 7E. For this flow rates, typical inner and outer diameter were 500 ± 31 µm and 656 ± 9 µm, with a coefficient of variation of 6.3 and 1.4%, respectively. The increase in the CV for the inner flow rate was attributed to inhomogeneous distribution of the inner phase across the parallel junctions. The presence of inbuilt filters, whilst successfully hindered the occlusion of the junctions with debris, can also cause preferential flow rates in certain junctions over others.

Figure 7C shows a stereoscope image of the microcapsules formed after the polymerisation. The double emulsions and the microcapsules are denser than the solution of PVA 5wt% used to collect the material, and therefore, it sinks during the polymerisation. Furthermore, no agglomeration of the capsules was observed. The size distribution of the capsules obtained over 7h are slightly broader than those obtained in shorter periods of time. This increased in size distribution is attributed to small variations in the flow rate over time, inhomogeneous distribution of fluid phases across the parallel junctions. Nevertheless, we find parallelised operation to yield good uniformity, with a CV for the outer diameter ~5.4% (Figure 7F). For this flow rates, the total throughput defined as the sum of inner and middle

Figure 7 - Double emulsion templates continuously formed for the production of microcapsules. (a) Optical microscopic image of the four microfluidic junctions in parallel producing double emulsions at flow rates of the inner, middle and outer phase were 82 µL min^{-1}, 130 µL min^{-1} and 400 µL min^{-1}, respectively. Scale-bar represents 500 µm. b) Optical microscopic image of the oil-in-oil-in-water double emulsion produced using junctions in parallel. Scale bar represents 400 µm. (c) stereoscope image of the microcapsules formed after photopolymerisation. Scale-bar represents 1000 µm. d) TGA indicating the core retention. E) Size distribution of the outer diameter of microcapsules, collected over 7h of reaction. F) Size distribution of the inner and outer diameter of double emulsions.

phases, is 12.72 mL.h^{-1} or 13.04 g.h^{-1}. By filtering the collected capsules after the production, the production yield was estimated to be 81 ± 1%. The main reason behind a yielding lower than 100%, is the mismatched density between the

inner and middle fluids, leading to a displacement of the core before the polymerisation. As a result, some of the capsules present a bowl-like shape, where the core escapes during Figure 7D), in which the amount of mineral oil retained inside of the capsules was estimated to be 44±21%. This equates to a production rate of 84.5 g in 8h, i.e., working hours, and ~0.25 kg per day. By parallelising more microfluidic chips in the same platform, further increases in production rate are possible. We estimate that a device containing 6 microfluidic chips in parallel, each one containing 4 junctions, could generate double emulsion at a rate of 1.5 kg per day.

Conclusions

High throughput of microcapsules using microfluidics were successfully produced for self-healing of cementitious materials. A microfluidic chip was designed in glass, with 4 channels in parallel. The modular approach enables the change in wettability for the production of double emulsions. Highly monodisperse double are formed using the channels in parallel, with a coefficient of variance below 2.5%. By varying the inner and middle flow rates, the shell thickness was successfully tailored to produce capsules with outer diameter ~600 µm and shell thickness between 50 and 127 µm. Furthermore, the flow rates were in the range of 30-180 $\mu L.min^{-1}$ for inner fluid and 32-120 $\mu L.min^{-1}$ for middle, resulting a production rate of 6-20 $g.h^{-1}$. Capsules with aqueous core were produced using trietanolamine as surfactant. Aiming at physically triggered self-healing, capsules with ethylene glycol phenyl ether acrylate (PEA) as shell material were produced, given the low tensile strength of the material. The capsule also showed very good interfacial bonding with the cement, and it was triggered upon crack formation. For the production of capsules for lab scale tests for self-healing, capsules were produced in continuously for 7h. The inner and outer diameter of the double emulsions were 500 ± 31 µm and 656 ± 9 µm, respectively. The coefficient of variation for the outer diameter of the capsules produced over 7h was 5.4% and the yielding of encapsulation was 81%.

The parallelised channels markedly amplify the production rate of double emulsions, without compromising the uniformity. By the addition of more microfluidic chip in parallel, we can further increase the throughput. This platform enables the production of emulsions for lab scale tests for self-healing.

Experimental

To produce the double emulsion, a microfluidic device with four flow-focusing channels in parallel, placed in a Telos device (Dolomite Microfluidics, UK), as shown in Figure 1. To obtain the suitable wettability for the production of double emulsion, the first part of the chip is hydrophobic while the second part is hydrophilic with a gasket connecting the two parts. At the first junction, where the inner flow is in contact with the middle flow, the junction is 300 µm deep and 310 µm wide. At the second junction, where the outer flow engulfs the previous two, the junction is 500 µm deep and 510 µm wide. The channel for the inner flow rate was 11.5 mm long, 240 µm width and depth of 80 µm; each of the 2 channels for the inlet of the middle flow was 20 mm long, 170 µm width and depth of 80 µm; and each of the 2 channels for the inlet of the outer flow was 27.5 mm length, 170 µm width and depth of 80 µm. In addition, the design also includes two sets of filters as a trapping point for debris, the first one with a depth of pores of 80 x170 µm and the second set of pores of 47x130 µm. The Telos platform is composed of a modular approach, with different modules being clamped together. The main inflow pathway presents a diameter of 1.5 mm and length of 27 mm (for each module), and branches out for individual modules through channels 23.5mm long and 1.0 mm of diameter. The inner fluid was injected using a syringe pump (Aladdin AL-1000) at the range of flow rates of 30-210 $\mu L.min^{-1}$; middle and outer fluids were injected using pressure pumps (Dolomite Microfluidics, UK) at typical flow rates of 30-150 $\mu L.min^{-1}$ and 300-430 $\mu L.min^{-1}$ for middle and outer fluids, respectively. Double emulsions with organic core were formed using mineral oil (light, Sigma Aldrich, density of 0.838 g mL-1, viscosity 29.3 mPa.s). For the aqueous core, a solution of triethanolamine (Sigma Aldrich) in water 1:1 was used as inner phase. The monomers used as precursor of the shell in the middle phase were trimethylolpropane ethoxylate triacrylate (ETMPTA, Sigma Aldrich, density 1.11 g mL-1, viscosity 73.3 mPa.s) and ethylene glycol phenyl ether acrylate (PEA, Sigma Aldrich) both containing 1 wt% of photoinitiator hydroxy-2-methylpropiophenone. For the outer/continuous phase, an aqueous solution with 5 wt% poly(vinyl alcohol) (PVA, MW 13000-23000, 87-89% hydrolysed, viscosity 4.99 mPa.s). The polymerisation of the shell took place using a UV-lamp (Omnicure, 50% opening) exposed over the collection tube shortly after the formation of the double emulsion droplets to minimise the effect of the density mismatch between the core and shell [44]. The resultant microcapsules were collected in an aqueous solution of 5 wt% PVA solution to prevent the agglomeration of the microcapsules during the polymerisation. To calculate the yielding during the 7h producing capsules, after every 1h, the container with capsules under the UV-light was removed and replaced by a new container with PVA 5 wt%. The capsules were filtered (filter paper no. 1, pore size 2.5 µm, diameter 42.5 mm, Whatman) and washed with water to remove any excess of PVA. The filtered material was then dried at room temperature for 24h, and the weight of the dried material was measured. To investigate the yielding, the weight of the dry capsules was divided by the sum of the weight of the inner and middle phases pumped for 1h

(calculated from the flow rates and density of the solutions). As this step was repeated every hour, an average yield was calculated for the 7h of production. The outer and inner diameter of the produced double emulsions and microcapsules were measured with an optical microscope (OM) (DM 2700 M, Leica, Germany) and a stereoscope (Leica, Germany). To assess the thermal stability and oil content, the microcapsules, mineral oil and polymerised ethylene glycol phenyl ether acrylate beads were analysed using thermogravimetric analysis (TGA, PerkinElmer STA6000) between 50 and 700 °C at a rate of 5 °C/min, under air atmosphere. For the investigation of the behaviour of the microcapsules in cement paste, microcapsules produced with mineral oil as a core and polymerised PEA as shell were mixed with Ordinary Portland cement (CEM I 42.5) provided by Heildelberg-UK and water (w/c=0.45). The mixture was then casted in oiled silicone moulds 10*10*50 mm^3. After 28 days of curing, the samples were broken, where it was possible to see the oil coming out of the microcapsules and leaking to the sample. To investigate the interfacial bonding between the capsule and cement paste, a scanning electron microscope (SEM, Evo LS15, Zeiss) was used.

Author Contributions

AA, LS – conceptualisation; LS – data curation, formal analysis, methodology, visualisation, writing; AA – resources, supervision.

Conflicts of interest

There are no conflicts to declare.

Acknowledgements

Financial support from EPSCR funded project RM4L Resilient Materials for Life (RM4L - EP/P02081X/1) is gratefully acknowledged.

References

1 N. De Belie, E. Gruyaert, A. Al-Tabbaa, P. Antonaci, C. Baera, D. Bajare, A. Darquennes, R. Davies, L. Ferrara, T. Jefferson, C. Litina, B. Miljevic, A. Otlewska, J. Ranogajec, M. Roig-Flores, K. Paine, P. Lukowski, P. Serna, J.-M. Tulliani, S. Vucetic, J. Wang and H. M. Jonkers, *Adv. Mater. Interfaces*, 2018, 1800074.

2 P. K. Mehta and P. J. M. Monteiro, *Concrete: Microstructure, Properties, and Materials, Fourth Edition*, McGraw-Hill Education, Fourth., 2014.

3 S. van der Zwaag, in *Self-Healing Materials*, ed. S. van der Zwaag, Springer Series in Materials Science, Dordrecht, vol. 100., 2007, pp. 1–18.

4 T. S. Qureshi and A. Al-Tabbaa, *Smart Mater. Struct.*, 2016, **25**, 084004.

5 M. Roig-Flores, F. Pirritano, P. Serna and L. Ferrara, *Constr. Build. Mater.*, 2016, **114**, 447–457.

6 S. Fan and M. Li, *Smart Mater. Struct.*, 2015, **24**, 015021.

7 D. Snoeck, L. Pel and N. De Belie, *Sci. Rep.*, 2020, **10**, 1–6.

8 Z. Li, L. R. de Souza, C. Litina, A. E. Markaki and A. Al-Tabbaa, *Mater. Des.*, 2020, **190**, 108572.

9 Z. Li, L. R. de Souza, C. Litina, A. E. Markaki and A. Al-Tabbaa, *Materials (Basel).*, 2019, **12**, 3872.

10 E. Tziviloglou, V. Wiktor, H. M. M. Jonkers and E. Schlangen, *Constr. Build. Mater.*, 2016, **122**, 118–125.

11 L. Tan, B. Reeksting, V. Ferrandiz-Mas, A. Heath, S. Gebhard and K. Paine, *Constr. Build. Mater.*, 2020, **257**, 119501.

12 J. Y. Wang, H. Soens, W. Verstraete and N. De Belie, *Cem. Concr. Res.*, 2014, **56**, 139–152.

13 B. Balzano, J. Sweeney, G. Thompson, C. L. Tuinea-Bobe and A. Jefferson, *Eng. Struct.*, 2021, **226**, 111330.

14 H. Huang, G. Ye and Z. Shui, *Constr. Build. Mater.*, 2014, **63**, 108–118.

15 A. Kanellopoulos, P. Giannaros and A. Al-Tabbaa, *Constr. Build. Mater.*, 2016, **122**, 577–593.

16 P. Giannaros, A. Kanellopoulos and A. Al-Tabbaa, *Smart Mater. Struct.*, 2016, **25**, 084005.

17 K. Van Tittelboom and N. De Belie, *Materials (Basel).*, 2013, **6**, 2182–2217.

18 X. Wang, Y. Huang, Y. Huang, J. Zhang, C. Fang, K. Yu, Q. Chen, T. Li, R. Han, Z. Yang, P. Xu, G. Liang, D. Su, X. Ding, D. Li, N. Han and F. Xing, *Constr. Build. Mater.*, 2019, **220**, 90–101.

19 M. Al-Ansari, A. G. Abu-Taqa, M. M. Hassan, A. Senouci and J. Milla, *Constr. Build. Mater.*, 2017, **149**, 525–534.

20 A. Beglarigale, Y. Seki, N. Y. Demir and H. Yazıcı, *Constr. Build. Mater.*, 2018, **162**, 57–64.

21 A. Kanellopoulos, P. Giannaros, D. Palmer, A. Kerr and A. Al-Tabbaa, *Smart Mater. Struct.*, 2017, **26**, 045025.

22 T. Han, X. Wang, D. Li, D. Li, F. Xing, J. Ren and N. Han, *Constr. Build. Mater.*, , DOI:10.1016/j.conbuildmat.2020.118009.

23 W. Mao, C. Litina and A. Al-Tabbaa, *Materials (Basel).*, 2020, **13**, 456.

24 Y. Ren, N. Abbas, G. Zhu and J. Tang, *Colloids Surfaces A Physicochem. Eng. Asp.*, , DOI:10.1016/j.colsurfa.2019.124347.

25 X. Wang, P. Sun, N. Han and F. Xing, *Materials (Basel).*, 2017, **10**, 20.

26 C. Litina, D. Palmer and A. Al-Tabbaa, *Eng. Res. Express*, 2021, **3**, 025015.

27 L. Y. Lv, H. Zhang, E. Schlangen, Z. Yang and F. Xing, *Constr. Build. Mater.*, 2017, **156**, 219–229.

28 W. Xiong, J. Tang, G. Zhu, N. Han, E. Schlangen, B. Dong, X. Wang and F. Xing, *Sci. Rep.*, 2015, **5**, 10866.

29 Y. Wang, G. Fang, W. Ding, N. Han, F. Xing and B. Dong, *Sci. Rep.*, 2015, **5**, 18484.

30 N. Xu, Z. Song, M. Z. Guo, L. Jiang, H. Chu, C. Pei, P. Yu, Q. Liu and Z. Li, *Cem. Concr. Compos.*, 2021, **118**, 103951.

31 L. Souza and A. Al-Tabbaa, *Constr. Build. Mater.*, 2018, **184**, 713–722.

32 P. W. Chen, G. Cadisch and A. R. Studart, *Langmuir*, 2014, **30**, 2346–50.

33 M. B. Romanowsky, A. R. Abate, A. Rotem, C. Holtze and D. A. Weitz, *Lab Chip*, 2012, **12**, 802–7.

34 T. Nisisako, T. Ando and T. Hatsuzawa, *Lab Chip*, 2012, **12**, 3426–3435.

35 H.-H. Jeong, Z. Chen, S. Yadavali, J. Xu, D. Issadore and D. Lee, *Lab Chip*, , DOI:10.1039/C8LC01267A.

36 A. Ofner, I. Mattich, M. Hagander, A. Dutto, H. Seybold, P. A. Rühs and A. R. Studart, *Adv. Funct. Mater.*, 2019, **29**, 1806821.

37 S. Nawar, J. K. Stolaroff, C. Ye, H. Wu, D. T. Nguyen, F. Xin and D. A. Weitz, *Lab Chip*, 2020, **20**, 147–154.

38 A. Chu, D. Nguyen, S. S. Talathi, A. C. Wilson, C. Ye, W. L. Smith, A. D. Kaplan, E. B. Duoss, J. K. Stolaroff and B. Giera, *Lab Chip*, 2019, **19**, 1808–1817.

39 S. A. Damiati, D. Rossi, H. N. Joensson and S. Damiati, *Sci. Rep.*, 2020, **10**, 19517.

40 S. L. Anna, N. Bontoux and H. A. Stone, *Appl. Phys. Lett.*, 2003, **82**, 364.

41 Y. Hennequin, N. Pannacci, C. P. de Torres, G. Tetradis-Meris, S. Chapuliot, E. Bouchaud and P. Tabeling, *Langmuir*, 2009, **25**, 7857–61.

42 P. W. Chen, R. M. Erb and A. R. Studart, *Langmuir*, 2012, **28**, 144–52.

43 A. Kanellopoulos, T. S. Qureshi and A. Al-Tabbaa, *Constr. Build. Mater.*, 2015, **98**, 780–791.

44 S. S. Datta, S.-H. Kim, J. Paulose, A. Abbaspourrad, D. R. Nelson and D. A. Weitz, *Phys. Rev. Lett.*, 2012, **109**, 134302.

45 T. Cubaud and T. G. Mason, *Phys. Fluids*, 2008, **20**, 053302.

46 J. K. Nunes, S. S. H. Tsai, J. Wan and H. A. Stone, *J. Phys. D. Appl. Phys.*, 2013, **46**, 114002.

47 J. Borrello, P. Nasser, J. C. Iatridis and K. D. Costa, *Addit. Manuf.*, 2018, **23**, 374–380.